HYDROTHERMAL PERFORMANCE EVALUATION OF SUPER HYDROPHOBIC SQUARE PIN FIN MINI CHANNEL HEAT SINK

by

Fazle HADI[a*], Hafiz Muhammad ALI[b,c*], and Faisal SIDDIQUE[d]

[a] Department of Mechanical Engineering,
University of Engineering and Technology,Taxila, Pakistan
[b] Mechanical Engineering Department, King Fahd University of Petroleum and Minerals,
Dhahran, Saudi Arabia
[c] Interdisciplinary Research Center for Renewable Energy and Power Systems (IRC-REPS),
King Fahd University of Petroleum and Minerals, Dhahran, Saudi Arabia
[d] Pakistan Institute of Engineering and Applied Sciences (PIEAS), Islamabad, Pakistan

Original scientific paper
https://doi.org/10.2298/TSCI210901009H

Efficient heat removal with less pressure drop is the focal point of research work in the field of thermal management systems. This research work is aimed to analyze inline square pin fin mini channel heat sink with superhydrophobic coating. The SiO_2 aqueous nanofluids with 0.01% and 0.02% volumetric concentration are used as heat transfer fluid. Data is attained at steady-state with a power input of 40 W, 55 W, and 70 W, flow rate of 300-700 ml per minute, and Reynolds number ranging from 400-1230. The test rig is authenticated by matching data of distilled water for a simple pin fin heat sink with the theoretical model of Tullius which matched the data well. Superhydrophobic mini channel heat sink gave a better performance with 25.23%, 21.8%, and 23.38% augmentation in Nusselt number and 33.19%, 30.5%, 31.1% reduction in pressure drop for distilled water, SiO_2 (0.01%) and SiO_2 (0.02%), respectively, as compared to the conventional pin fin mini channel heat sink. The nutshell of this experimental work is magnification in heat transfer with a reduction in pressure drop.

Keywords: *pin fin, superhydrophobic, heat transfer, pressure drop, mini channel*

Introduction

The fast technological growth in the near past has compelled researchers to find efficient and smart heat removal techniques. Safe and consistent working of all electronics and other automatized devices depends upon an efficient cooling system. The conventional ways of heat removal and heat transfer fluids (HTF) cannot overcome the problems and, therefore, advanced systems with better thermal management are the utmost requirement of the miniaturized systems. The confined thermophysical properties of conventional HTF offer a barrier and the researchers are obligated to find the other way out. Maxwell [1] used microscale particles to enhance the thermophysical properties of the base fluids. These particles suffered the problem of agglomeration and limitations in micro-sized channels. Choi and Eastman [2] introduced nanoparticles and resolved the issue of agglomeration. Since then, nanofluids are reviewed by different researchers [3-6] regarding their fabrication, stability, and usage.

[*] Corresponding authors, e-mail: fazlehadi@yahoo.com, hafiz.ali@kfupm.edu.sa

Nanoparticles of different natures like metal particles, metal oxide, graphite, diamond, simple and coated carbon nanotubes*, etc.* are generally used for the synthesis of nanofluids [7, 8]. In the recent past, a lot of numerical and experimental work has been carried out to analyze the thermal capabilities of mono and hybrid nanofluids [9] in mini and micro-channels [10-14]. Experimental analysis of aqueous alumina nanofluid is performed by Nguyen *et al.* [15] with different particle sizes and concluded that nanoparticles with smaller sizes performed well. CuO and water nanofluid is investigated by Selvakumar and Suresh [16] and recorded a 20% rise in heat transfer with an increase in pressure losses. Nanofluids have also been recommended for use in low to medium-temperature solar collectors [17] and reflectors [18] to enhance heat transfer.

Pressure drop variation in micro-channels is based on the viscosity of nanofluids which is dependent on the gap between the surfaces [19]. Jang *et al.* [20] and Chevalier *et al.* [21] have studied these effects with the conclusion that micro-channels are responsible for high shearing rate

$$\gamma\left(\text{shearing rate}\right)=\frac{v}{x}$$

where v is the velocity and x – the distance between the high and low speed layer which is smaller in micro-channels and give rise to higher shear rate. Shear stress increases with the rise in shearing rate as shown in fig. 3 by Nghe *et al.* [22]. A collision between particles occurs due to unequal velocities in different strata under the shearing motions which affect the instantaneous viscosity of the fluid in the micro-channel. Based on these facts, it is concluded by Chevalier *et al.* [21] that micro-channels cause a high shear rate which affects the viscosity of nanofluids due to enhanced shear motion collision.

Ijam and Saidur [23] studied SiC-water and TiO_2-water nanofluids using a mini channel heat sink (MnCHS) and noted 12.44% and 9.99% turn-wise enhancement in thermal conductivity. A Micro-channel heat sink with staggered square pin fin geometry using water was studied by Liu *et al.* [24] and an increase in heat transfer with the penalty of pressure drop is recorded. Besides the use of mini/micro-channels and nanofluids, superhydrophobic surfaces can also be a good introduction the field of thermal management. In this regard, surfaces are modified to make them either superhydrophobic with a contact angle greater than 150^o or superhydrophilic having a contact angle less than 10^o [25-27]. Modification techniques are developed for a series of materials like Cu [28], Al [29], Mg [30], Si [31], and Au [32]*, etc.* In the past, superhydrophobic surfaces have been used in the area of anti-icing [33], drag reduction [25], self-cleaning [34] and increase in resistance against corrosion [30]*, etc.* but single-phase heat transfer in a MnCHS with superhydrophobic surfaces has rarely been addressed.

Keeping in view the available literature, it is concluded that the hydrothermal performance of superhydrophobic MnCHS and especially with square pin fin geometry has not been evaluated so far. Therefore, this research is focused on the hydrothermal performance comparison of superhydrophobic inline square pin fin MnCHS with conventional inline square pin fin MnCHS using the same working parameters and working fluids.

Methodology

Experimental test rig

The experimental set-up, used in this research, is photographically shown in fig. 1. It comprises a reservoir to accumulate the HTF, a high pressure DC pump (China), a precise needle valve (3 RE-02 IPH, Japan), a flow meter (FS-3, Regal Japan), a radiator (Thermaltake TT-1225 China), filter (Pakistan), inline square pin fin MnCHS (IST California), three cartridge heaters, each of 200 W (Pakistan), six thermocouples (5TC-K1-24-2M, Omega USA), a differential pressure transducer (YOKOGAWA, Japan), variable power supply (6657A Keysight USA),), controlled output DC power supply (U8032A Keysight, USA), Data logger (Agilent USA), and a Desktop computer.

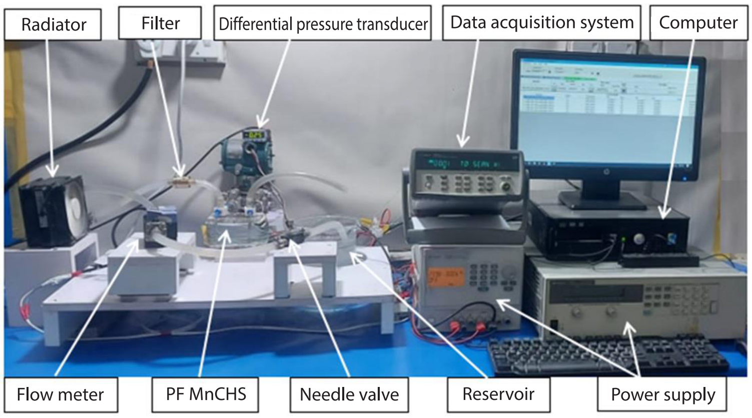

Figure 1. Experimental set-up

A high pressure DC pump (China) is used to pass HTF through the experimental loop. A precise needle valve is used to regulate and control the flow. The volumetric flow rate is recorded with the help of a flow meter and through physical measurement using a precise flask before and after starting of each experiment. The inlet temperature is controlled through a double fan radiator. Also, a micron-sized filter is used in the loop before the inlet of the heat sink to avoid any foreign particles from entering the mini channels.

An accurately calibrated differential pressure transducer is installed in the loop between the inlet and outlet of MnCHS to measure pressure losses of HTF during flow through the MnCHS. The high and low pressure ports of the transducer are connected to the inflow and outflow ports of MnCHS correspondingly. The MnCHS are made of copper having twelve rows of inline square pin fins with cross-sectional area of one mm as shown in fig. 2.

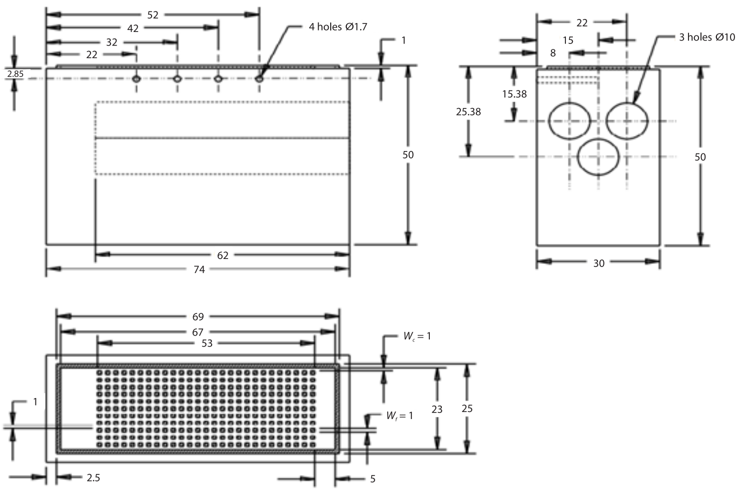

Figure 2. Detailed drawing of inline square pin fin MnCHS

A total of six thermocouples *i.e.* one at the inlet, one at the outlet, and four at 2.87 mm from the base of the channels, are installed to measure the temperature. These thermocouples are connected to the data logger. The inlet, outlet, and wall base temperatures are recorded after every five seconds at steady flow.

The pressure drop of HTF, during flow through MnCHS, is recorded through a differential pressure transmitter with an accuracy of 0.1 mbar. Three cartridge heaters are inserted in the heat sink to provide uniform heat to the heat sink. These heaters are connected to a variable DC power supply. The HTF was transferred to the reservoir after passing through the pin fin MnCHS.

Synthesis of nanofluid

Nanofluid is one of the most essential element of experimental analysis. The SiO_2 aqueous nanofluids with 0.01% and 0.02% volumetric concentration are synthesized by two-step technique [35, 36]. The SiO_2 nanoparticles (diameter = 20 nm) were procured from Nano-Structured and Amorphous Material USA. Nanofluid was homogenized with the help of a homogenizer (IKA T50 D Germany) for 1-1/2 hours. Maxtrix, DAIHAN Scientific USA stirrer has been used to stir nanofluid for two hours to break the clusters. The nanofluids were ultra-sonicated for six hours using a sonication bath (WUC-A22H DAIHAN Sci. Korea) for stable suspension of nanoparticles. The electrical conductivity of nanofluidswas assessed with the help of Danver Intr.-250 USA, before and after usage, to check stability of the nanofluid. Electrical conductivity remained the same *i.e.* 8.8 μS/cm which confirmed stability of the nanofluid. Also, visual inspection was carried out after 24 hours of sonication and no sedimentation of particles was visualized, as shown in fig. 3.

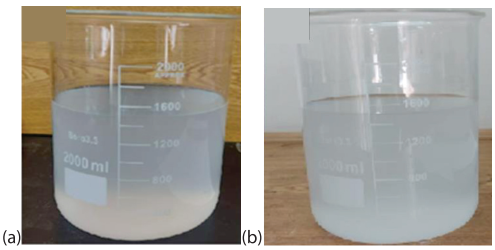

Figure 3. The SiO_2 nanofluid (a) after sonication and (b) after 24 hours

Superhydrophobic coating

The main focus of the present research work is to analyze the hydrothermal performance of inline square pin fin superhydrophobic MnCHS using distilled water and SiO_2 aqueous nanofluids with 0.01% and 0.02% concentrations and compare the results with conventional (without coating) MnCHS. Two numbers of inline square pin fin copper MnCHS were manufactured with the help of a computer numerical control milling machine. One MnCHS was sent to Integrated Surface Technology (IST) California, USA for superhydrophobic coating as shown in fig. 4. The IST has used the Modified Repellix-2 technique for the required super hydrophobic coating with a contact angle of 167° and a coating thickness of 60-100 nm.

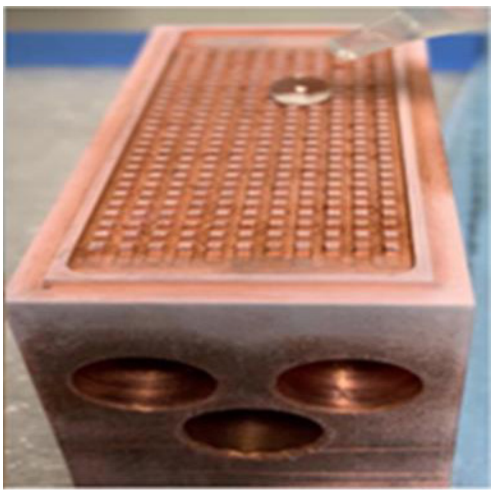

Figure 4. Superhydrophobic square pin fin MnCHS

Thermophysical properties measurement

The basic thermophysical properties of nanofluids like volume fraction of nanofluids/nanoparticles, density, viscosity, and thermal conductivity are calculated using mathematical equations.

The volume fraction of nanoparticles, φ, is found:

$$\varphi = \frac{w_{\text{np}}\rho_{\text{bf}}}{\left[\rho_{\text{np}}\left(1 - w_{\text{np}}\right) + w_{\text{np}}\rho_{\text{bf}}\right]} \tag{1}$$

where w_{np} is weight and ρ_{np} is the density of the nanoparticles.

Evaluation of nanofluid density, ρ_{nf}:

$$\rho_{\text{nf}} = \varphi\rho_{\text{np}} + \left(1 - \varphi\right)\rho_{\text{bf}} \tag{2}$$

The nanofluid viscosity, μ_{nf}, is calculated with the help of Corcione [37]:

$$\mu_{\text{nf}} = \frac{\mu_{\text{bf}}}{1 - 34.87\left(\dfrac{d_{\text{np}}}{d_{\text{bf}}}\right)^{-0.3}\varphi^{1.03}} \tag{3}$$

where d_{np} is the diameter of the nanoparticle and d_{bf} – the diameter of the distilled water molecule (base fluid) and is found:

$$d_{\text{bf}} = 0.1\left[\frac{6M}{N\pi\rho_{\text{bf}}}\right]^{1/3} \tag{4}$$

where M = 18 g/mole (Molecular weight of water) and N = Avogadro number ($6.02\cdot10^{23}$).

Hamilton and Cross model [38] is used to find out thermal conductivity of nanofluid, K_{nf}:

$$\frac{K_{\text{nf}}}{K_{\text{bf}}} = \left[\frac{K_{\text{np}} + \left(n-1\right)K_{\text{bf}} - \left(n-1\right)\varphi\left(K_{\text{bf}} - K_{\text{nf}}\right)}{K_{\text{np}} + \left(n-1\right)K_{\text{bf}} + \varphi\left(K_{\text{bf}} - K_{\text{nf}}\right)}\right] \tag{5}$$

where $n = 3/\psi$ and ψ represents sphericity of nanoparticle.

The $C_{p,\text{nf}}$ (specific heat capacity) of nanofluid is assessed:

$$C_{p,\text{nf}} = \frac{\varphi\rho_{\text{np}}C_{p,\text{np}}}{\rho_{\text{nf}}} + \frac{\left(1-\varphi\right)\rho_{\text{bf}}C_{p,\text{bf}}}{\rho_{\text{nf}}} \tag{6}$$

Measurement of convective heat transfer

Rate of heat transfer, Q, by nanofluid:

$$Q = \dot{m}C_p\left(T_{\text{out}} - T_{\text{in}}\right) \tag{7}$$

Thermal efficacy of HTF and heat sink is linked with HTC which is assessed:

$$h = \frac{\dot{m}C_p\left(T_{\text{out}} - T_{\text{in}}\right)}{A_{\text{es}}\left(LMTD\right)} \tag{8}$$

The A_{eff} is the effective area of the MnCHS and is evaluated:

$$A_{\text{eff}} = N_{\text{ch}}L_{\text{s}}\left(2h_{\text{f}} + w_{\text{ch}}\right) \tag{9}$$

where N_{ch} = Number of channels = 12.

The LMTD (Log mean temperature difference) is determined:

$$LMTD=\frac{\left(T_\mathrm{w}-T_\mathrm{in}\right)-\left(T_\mathrm{w}-T_\mathrm{out}\right)}{\ln\dfrac{\left(T_\mathrm{w}-T_\mathrm{in}\right)}{\left(T_\mathrm{w}-T_\mathrm{out}\right)}} \tag{10}$$

where T_w is measured at 2.85 mm below the channel base, H_w. It may be estimated by Fourier's law, assuming that heat transfer between thermocouples and sink is 1-D:

$$T_\mathrm{w}=T_\mathrm{thc}-\left(\frac{QH_\mathrm{w}}{K_\mathrm{s}A_\mathrm{w}}\right) \tag{11}$$

Equation (12) is used to assess the value of Nusselt number, Nu, whereas eq. (13) is used to calculate hydraulic diameter, d_h, of the channels:

$$\mathrm{Nu}=\frac{hd_\mathrm{h}}{k} \tag{12}$$

$$d_\mathrm{h}=\frac{4A_\mathrm{cc}}{2h_\mathrm{f}+w_\mathrm{cc}} \tag{13}$$

The values calculated from the experimental data are compared with the values predicted by the correlation of Tullius [39]:

$$\overline{\mathrm{Nu}}=0.0937\left(\frac{S_L}{d_{\mathrm{h_f}}}\right)^{0.2}\left(\frac{S_t}{d_{\mathrm{h_f}}}\right)^{0.2}\left(\frac{h_\mathrm{f}}{d_{\mathrm{h_f}}}\right)^{0.25}\left(1+\frac{d_\mathrm{h}}{d_{\mathrm{h_f}}}\right)^{0.4}\mathrm{Re}_f^{0.6}\mathrm{Pr}^{0.36}\left(\frac{\mathrm{Pr}}{\mathrm{Pr_s}}\right)^{0.25} \tag{14}$$

Thermal resistance, R_th, anticipates thermal efficacy of the sink and HTF, and is evaluated:

$$R_\mathrm{th}=A_\mathrm{cc}\left(\frac{LMTD}{Q}\right) \tag{15}$$

Pressure drop and pumping power

Pressure drop, ΔP, is recorded using a differential pressure transducer. It may be calculated:

$$\Delta P=f\frac{L}{D_\mathrm{h}}\left(\frac{\rho V_m^2}{2}\right) \tag{16}$$

Experimental data is compared with Steinke and Kandlikar [40] correlation given:

$$\Delta P=\frac{2\left(f\mathrm{Re}\right)\mu VL_\mathrm{eff}}{\left(d_\mathrm{h}\right)^2}+\frac{k\left(x\right)\rho\overline{V}^2}{2} \tag{17}$$

where $k(x)$ is the

$$\text{Hagenbach factor}=\left(f_\mathrm{app}-f_\mathrm{FD}\right)\frac{4x}{d_\mathrm{h}}$$

The required pumping power is evaluated:

$$P_p=\dot{V}\Delta P \tag{18}$$

Results and discussion

Validation

The experimental test rig is developed locally and validated by matching experimental data with the data assessed through the theoretical models. In this connection, results are recorded for distilled water at 40 W using conventional straight MnCHS. These results are compared with the theoretical model of Tullius *et al*. [39] for Nusselt number and Steinke and Kandlikar [40] for pressure drop as shown in figs. 5(a) and 5(b), respectively. It is noted that both the data followed the same trend and experimental results matched the theoretical models well with a maximum deviation of 6.9% for Nusselt number and 7.5% for pressure drop.

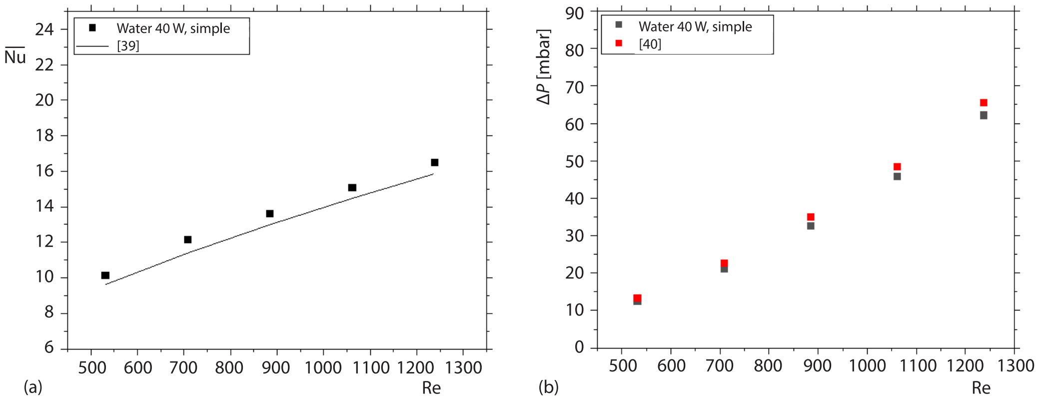

Figure 5. Experimental data of water theoretical model; (a) [39] for $\overline{\mathrm{Nu}}$ and (b) [40] for ΔP

Superhydrophobic vs. conventional mini channel heat sink

Effect of Super hydrophobic coating on Nusselt number

Experimental results are plotted against the Reynolds number as shown in fig. 6 for water and figs 8(a)-8(c) for SiO_2. The plots show that the Nusselt number is reliant on mass-flow rate and rises with the rise in Reynolds number for all the nanofluids and both types of heat sinks. Power input has affected the Nuesselt number significantly. In the case of water, the Reynolds number does not change with an increase in power input at the same mass-flow rate as viscosity remains the same. Super-hydrophobic MnCHS gave 25.23%, 21.8%, and 23.38% greater Nusselt number than conventional MnCHS for distilled water, SiO_2 (0.01%) and SiO_2 (0.02%) nanofluids, respectively. The escalation in thermal performance is due to repelling property of superhydrophobic surfaces. The repellence enhances shear-thinning [41] and demolishes the thermal boundary-layer referred to as the heat transfer barrier. Therefore, fresh layers of working fluids get more opportunities to come in contact with the heated surface resulting in greater convectional heat transfer. The churning effect and Brownian motion are also contributing to enhance Nusselt number.

Effect of superhydrophobic coating on pressure drop

The experimental pressure drop values are plotted against Reynolds number for water and SiO_2 with 0.01% and 0.02% volumetric concentration as shown in figs. 7 and 9(a)-9(c). Pressure drop is amplified with the rise in mass-flow rate for all the fluids and both types of the MnCHS. Pressure drop does not vary with the power input because the viscosity of all the

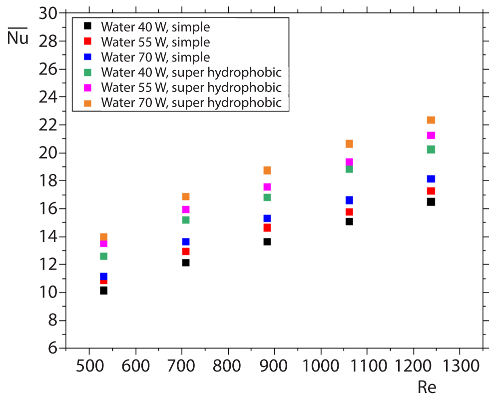

Figure 6. The Nu *vs.* Re of water

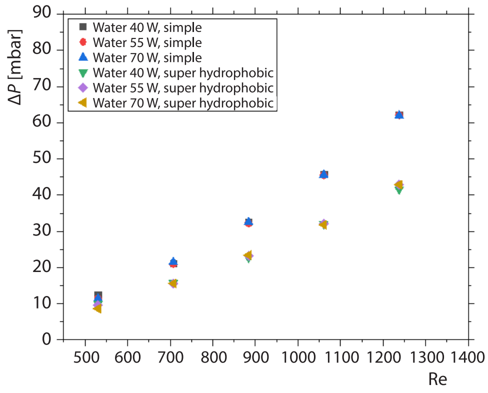

Figure 7. The ΔP *vs.* Re of water

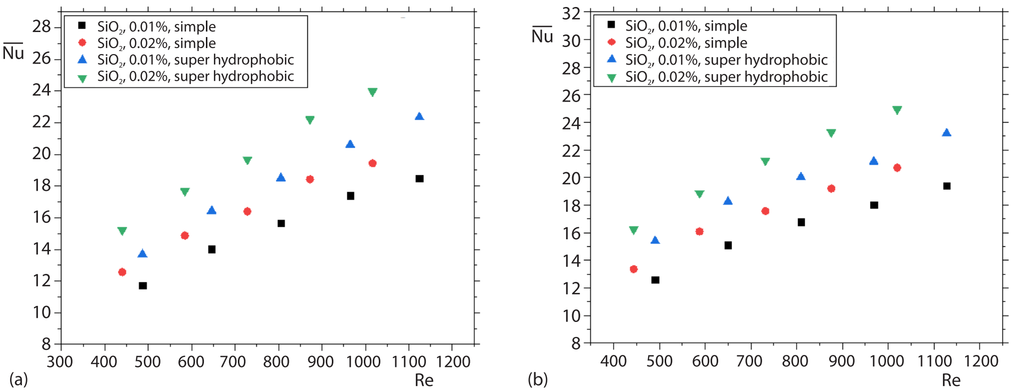

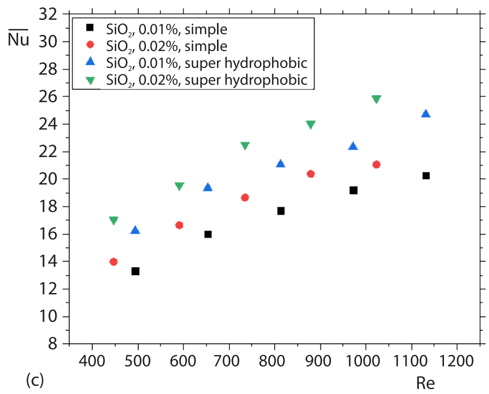

Figure 8. The Nu *vs.* Re of SiO_2; (a) *Q* = 40 W, (b) *Q* = 55 W, and (c) *Q* = 70 W

working fluids is not significantly affected due to the very small concentration. Keeping in view the main focus of this research, the results, shown in. Figures 7 and 9(a)-9(c) illustrate that superhydrophobic coating has a tremendous effect on pressure drop and pumping power and a reduction of 33.19%, 30.5%, 31.1% in pressure drop and pumping power is noted for superhydrophobic MnCHS as compared to conventional MnCHS for distilled water, SiO_2 (0.01%) and SiO_2 (0.02%) nanofluids accordingly at the same Reynolds number.

The decline in pressure drop using super hydrophobic MnCHS is due to the hydrophobicity of the surfaces. It decreases surface drag, friction, velocity gradient, and entry effect. It produces greater slip length. A slip length of more than 200 μ is noted by Choi *et al.* [42]. Secondly, the shear thinning of fluids may generate a heterogeneous layer near the solid surface which causes greater apparent slip [41].

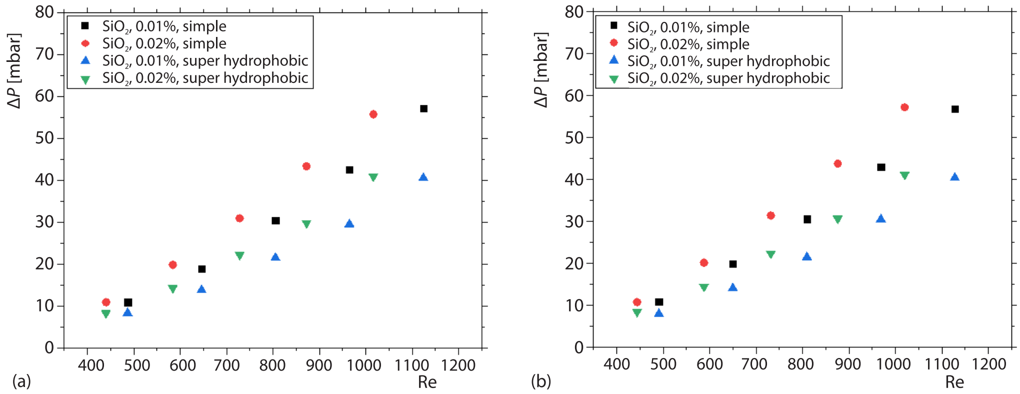

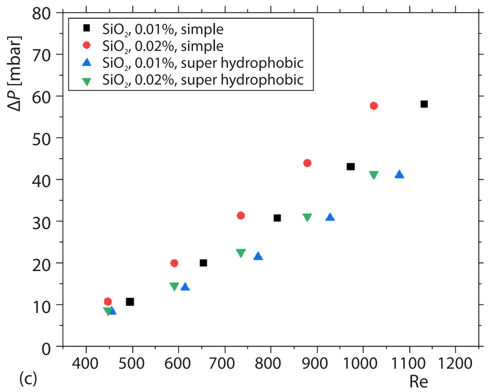

Figure 9. The ΔP *vs.* Re of SiO_2; (a) Q = 40 W, (b) Q = 55 W, and (c) Q = 70 W

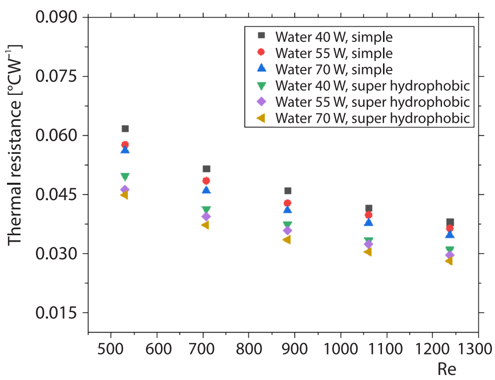

Figure 10. The R_{th} *vs.* Re of water

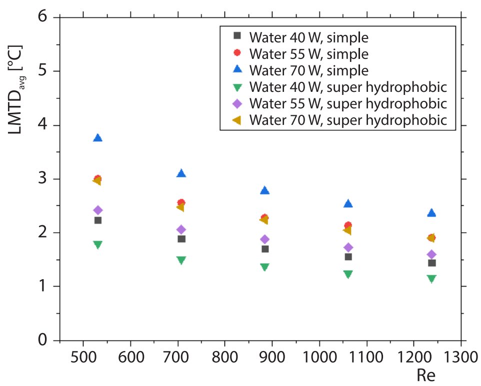

Figure 11. The LMTD *vs.* Re of water

Effect of superhydrophobic coating on thermal resistance

Experimental data of thermal resistance for both types of MnCHS and all HTF are plotted against the Reynolds number as shown in fig. 10 for water and figs. 12(a)-12(c) for SiO_2. Thermal resistance dwindles with amplification in Reynolds number, as expected, and rises with the increase in power input. Nanofluids gave better performance than distilled water at the same Reynolds number for both types of MnCHS. Superhydrophobic MnCHS appeared as a good performer than the conventional one with an edge of 20.09%, 17.9%, and 18.9% lower R_{th} for water, SiO_2 (0.01%), and SiO_2 (0.02%) nanofluids turnwise.

In the case of superhydrophobic surfaces, the thermal boundary-layer is either reduced to a minimum value or demolished. Therefore, fresh currents of fluid are given more chances to touch the heated surface and enhance the cooling of the surface. This causes amplified thermal performance and produces shear-thinning which reduces thermal resistance.

Effect of superhydrophobic coating on LMTD

The LMTD predicts the thermal performance of a system. It is based on wall base temperature and thermal resistance. In this experimental work, wall base temperature and R_{th} are reduced by introducing superhydrophobic coating on the active surfaces of MnCHS. Figures 11 and 13(a)-13(c) are plotted between the experimental values of LMTD and Reynolds number for water and SiO_2 correspondingly. The graphs depict that LMTD decreases with an increase in Reynolds number based on the natural phenomenon.

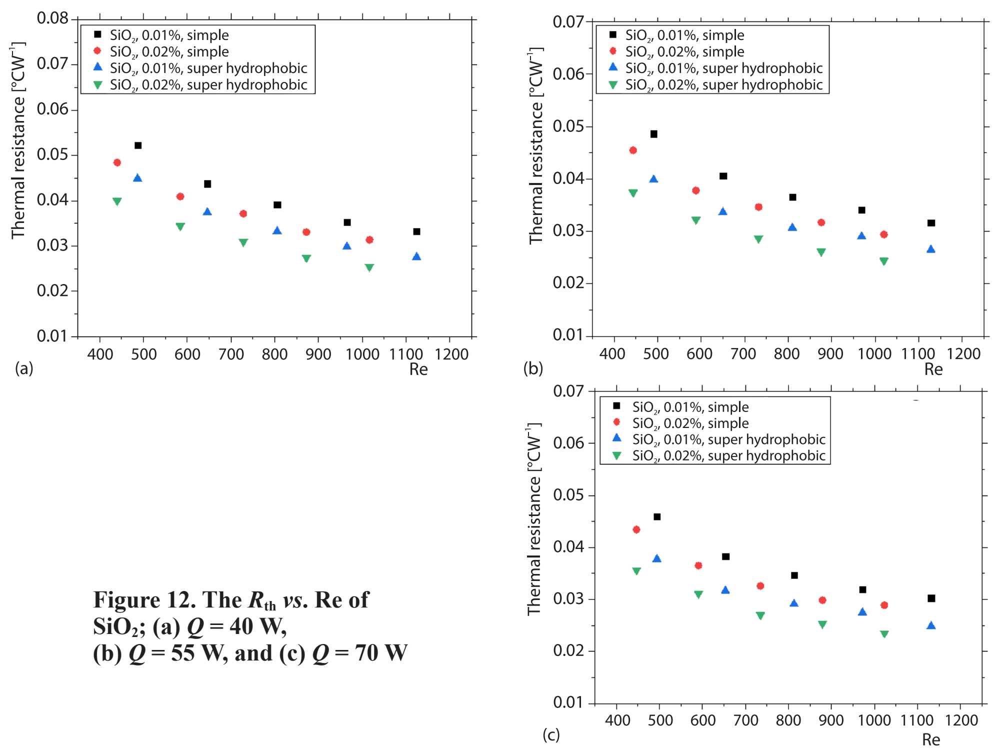

Figure 12. The R_{th} *vs.* Re of SiO_2; (a) Q = 40 W, (b) Q = 55 W, and (c) Q = 70 W

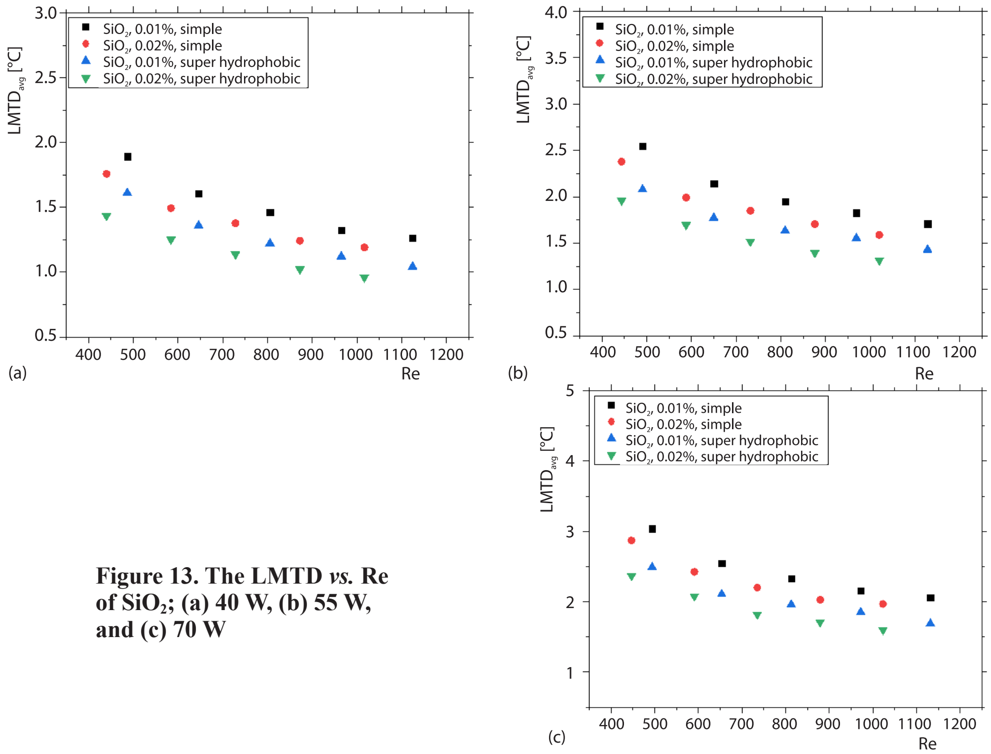

Figure 13. The LMTD *vs.* Re of SiO_2; (a) 40 W, (b) 55 W, and (c) 70 W

The superhydrophobic coating has a tremendous effect on LMTD and it is decreased by 20.92% for water, 18.09% for SiO_2 (0.01%), and 19.39% for SiO_2 (0.02%) nanofluids as compared to conventional MnCHS.

The LMTD is reduced due to enhanced convectional heat transfer caused by superhydrophobic surfaces.

Conclusions

Results are compiled with the following conclusions.

- Superhydrophobic mini channel heat sink performed exclusively better than the conventional one with an edge of 25.23%, 21.8%, and 23.38% augmentation in Nusselt number for distilled water, SiO_2 (0.01%), and SiO_2 (0.02%) nanofluids, respectively at the same working parameters.
- Pressure drop for the superhydrophobic MnCHS is recorded to be 33.19%, 30.5%, and 31.1% lower than the conventional MnCHS for distilled water, SiO_2 (0.01%) and SiO_2 (0.02%) nanofluids, respectively.
- Thermal resistance of superhydrophobic MnCHS is noted as 20.09% for distilled water, 17.9% for SiO_2 (0.01%) and 18.9% for SiO_2 (0.02) nanofluids lower than conventional MnCHS with 0.024°C as the minimum value of thermal resitance for SiO_2 (0.02%) nanofluid.
- The LMTD of superhydrophobic MnCHS is charted as 20.92%, 18.09%, 19.39% lower than the conventional MnCHS for distilled water, SiO_2 (0.01%) and SiO_2 (0.02%) nanofluids, respectively. The lowest LMTD value of 1.04°C is noted for SiO_2 (0.02%).

- The overall hydro-thermal performance of the superhydrophobic inline square pin fin mini channel heat sink has been fabulous with amplified heat transfer and reduced pressure drop.

Nomenclature

C_p – specific heat, [Jkg^{-1}°C^{-1}]
D_h – hydraulic diameter, [m]
dh – clearance of the channel, [m]
f – friction factor
h – co-efficient of convective heat transfer, [Wm^{-2}°C^{-1}]
h_b – base thickness of heat sink, [m]
h_f – fin height, [m]
H_w – distance from sink base to the thermocouple, [m]
L – length of the heat sink, [m]
$\dot{m}$ – mass-flow rate, [kgs^{-1}]
N_{ch} – number of channels
n – empirical shape factor
Nu – Nusselt number
ΔP – pressure drop, [mbar]
P – perimeter, [m]
R_{th} – thermal resistance
w_{c} – channel width, [mm]
w_{f} – fin width, [mm]

Greek symbols

α – mini channel aspect ratio
μ – viscosity, [kg(ms^{-1})$^{-1}$]
φ – volume fraction
ρ – density, [kgm^{-3}]
ψ – particle roundness

Subscripts

cc – channel cross-section
$\mathrm{c_f}$ – fin cross-section
f – fin
nf – nanofluid
ch – channel
np – nanoparticle
r – room temperature
tc – thermocouple
w – wall

Reference

[1] Maxwell, J. C., *A Treatise on Electricity and Magnetism*, Clarendon Press, Oxford, UK, 1873, Vol. 1
[2] Choi, S. U., Eastman, J. A., *Enhancing Thermal Conductivity of Fluids with Nanoparticles*, Argonne National Lab., Lemont, Ill., USA, 1995
[3] Sadeghinezhad, E., *et al.*., *A Comprehensive Review on Graphene Nanofluids: Recent Research, Development, and Applications, Energy Conversion and Management*, *111* (2016), Mar., pp. 466-487
[4] Leong, K., *et al.*, *An Overview on the Current Application of Nanofluids in the Solar Thermal Collector and Its Challenges*, *Renewable and Sustainable Energy Reviews*, *53* (2016), Jan., pp. 1092-1105
[5] Huminic, G., Huminic, A., *Application of Nanofluids in Heat Exchangers: A Review, Renewable and Sustainable Energy Reviews*, *16* (2012), 8, pp. 5625-5638
[6] Solangi, K., *et al.*, *A Comprehensive Review of Thermo-Physical Properties and Convective Heat Transfer to Nanofluids, Energy*, *89* (2015), Sept., pp. 1065-1086
[7] Babu, J. R., *et al.*, State-of-Art Review on Hybrid Nanofluids, *Renewable and Sustainable Energy Reviews*, *77* (2017), Sept., pp. 551-565
[8] Said, Z., *et al.*, *Synthesis, Stability, Thermophysical Properties and AI Approach for Predictive Modelling of Fe_3O_4 Coated MWCNT Hybrid Nanofluids*, *Journal of Molecular Liquids*, *340* (2021), 117291
[9] Cakmak, N. K., *et al.*, *Preparation, Characterization, Stability, and Thermal Conductivity of rGO-Fe_3O_4-TiO_2 Hybrid Nanofluid: An Experimental Study*, *Powder Technology*, *372* (2020), July, pp. 235-245
[10] Asthana, A., *et al.*, *Significant Nusselt Number Increase in Micro-Channels with a Segmented Flow of Two Immiscible Liquids: An Experimental Study,* International Journal of Heat and Mass Transfer, *54* (2011), 7-8, pp. 1456-1464
[11] Tokit, E. M., *et al.*, *Thermal Performance of Optimized Interrupted Micro-Channel Heat Sink (IMCHS) Using Nanofluids*, *International Communications in Heat and Mass Transfer*, *39* (2012), 10, pp. 1595-1604
[12] Godson, L., *et al.*, Enhancement of Heat Transfer Using Nanofluids – An Overview, *Renewable and Sustainable Energy Reviews*, *14* (2010), 2, pp. 629-641
[13] Kanti, P., *et al.*, Entropy Generation and Friction Factor Analysis of Fly Ash Nanofluids Flowing in a Horizontal Tube: Experimental and Numerical Study, *International Journal of Thermal Sciences*, *166* (2021), 106972

[14] Said, Z., *et al.*, Recent Advances on the Fundamental Physical Phenomena behind Stability, Dynamic Motion, Thermophysical Properties, Heat Transport, Applications, and Challenges of Nanofluids, *Physics Reports*, *946* (2022), Feb., pp. 1-94
[15] Nguyen, C. T., *et al.*, Heat Transfer Enhancement Using Al_2O_3-Water Nanofluid for an Electronic Liquid Cooling System, *Applied Thermal Engineering*, *27* (2007), 8-9, pp. 1501-1506
[16] Selvakumar, P., Suresh, S., Convective Performance of CuO-Water Nanofluid in an Electronic Heat Sink, *Experimental Thermal and Fluid Science*, *40* (2012), July, pp. 57-63
[17] Said, Z., *et al.*, Recent Advances on Nanofluids for Low to Medium Temperature Solar Collectors: Energy, Exergy, Economic Analysis, and Environmental Impact, *Progress in Energy and Combustion Science*, *84* (2021), 100898
[18] Said, Z., *et al.*, Heat Transfer, Entropy Generation, Economic and Environmental Analyses of Linear Fresnel Reflector Using Novel rGO-Co_3O_4 Hybrid Nanofluids, *Renewable Energy*, *165* (2021), Mar., pp. 420-437
[19] Pipe, C. J., *et al,* High Shear Rate Viscometry, *Rheologica Acta*, *47* (2008), 5-6, pp. 621-642
[20] Jang, S. P., *et al.*, Particle Concentration and Tube Size Dependence of Viscosities of Al_2O_3-Water Nanofluids Flowing through Micro and Mini Tubes, *Applied Physics Letters*, *91* (2007), 24, 243112
[21] Chevalier, J., *et al*., Rheological Properties of Nanofluids Flowing through Micro-Channels, *Applied Physics Letters*, *91* (2007), 23, 233103
[22] Nghe, P., *et al*., High Shear Rheology of Shear Banding Fluids in Micro-Channels, *Applied Physics Letters*, *93* (2008), 20, 204102
[23] Ijam, A., Saidur, R., Nanofluid as a Coolant for Electronic Devices (Cooling of Electronic Devices), *Applied Thermal Engineering*, *32* (2012), 1, pp. 76-82
[24] Liu, M., *et al*.., Experimental Study on Liquid-Flow and Heat Transfer in Micro Square Pin Fin Heat Sink, *International Journal of Heat and Mass Transfer*, *54* (2011), 25-26, pp. 5602-5611
[25] Shirtcliffe, N. J., *et al*., Superhydrophobic Copper Tubes with Possible Flow Enhancement and Drag Reduction, ACS Applied Materials and Interfaces, *1* (2009), 6, pp. 1316-1323
[26] McDonald, B. T., Cui, T., Superhydrophilic Surface Modification of Copper Surfaces by Layer-by-Layer Self-Assembly and Liquid Phase Deposition of TiO_2 Thin Film, *Journal of Colloid and Interface Science*, *354* (2011), 1, pp. 1-6
[27] Liu, T., *et al.*, Super-Hydrophobic Surfaces Improve the Corrosion Resistance of Copper in Seawater, *Electrochimica Acta*, *52* (2007), 11, pp. 3709-3713
[28] Qian, B., Shen, Z., Fabrication of Superhydrophobic Surfaces by Dislocation-Selective Chemical Etching on Aluminum, Copper, and Zinc Substrates, *Langmuir*, *21* (2005), 20, pp. 9007-9009
[29] Cao, L., *et al*., Anti-Icing Superhydrophobic Coatings, *Langmuir*, *25* (2009), 21, pp. 12444-12448
[30] Wang, Y., *et al*., Super-Hydrophobic Surface on Pure Magnesium Substrate by Wet Chemical Method, *Applied Surface Science*, *256* (2010), 12, pp. 3837-3840
[31] Guo, L., *et al*., Stable Superhydrophobic Surfaces over a Wide pH Range, *Applied Surface Science*, *254* (2008), 7, pp. 2158-2161
[32] Yu, X., *et al*., Surface Gradient Material: From Superhydrophobicity to Super Hydrophilicity, *Langmuir*, 22 (2006), 10, pp. 4483-4486
[33] Kulinich, S., *et al*., Superhydrophobic Surfaces: Are they Really Ice-Repellent, *Langmuir*, *27* (2010), 1, pp. 25-29
[34] Bhushan, B., *et al*., Micro-, nanoand Hierarchical Structures for Superhydrophobicity, Self-Cleaning and Low Adhesion, Philosophical Transactions of the Royal Society A: *Mathematical, Physical and Engineering Sciences*, *367* (2009), 1894, pp. 1631-1672
[35] Li, Y., et al., A Review on the Development of Nanofluid Preparation and Characterization, *Powder Technology*, *196* (2009), 2, pp. 89-101
[36] Li, X., *et al*., Evaluation on Dispersion Behavior of the Aqueous Copper Nanosuspensions, *Journal of Colloid and Interface Science*, *310* (2007), 2, pp. 456-463
[37] Corcione, M., Rayleigh-Benard Convection Heat Transfer in Nanoparticle Suspensions, *International Journal of Heat and Fluid-Flow*, *32* (2011), 1, pp. 65-77
[38] Hamilton, R. L., Crosser, O., Thermal Conductivity of Heterogeneous Two-Component Systems, *Industrial & Engineering Chemistry Fundamentals*, *1* (1962), 3, pp. 187-191
[39] Tullius, J., *et al.*, Optimization of Short Micro Pin Fins in Minichannels, *International Journal of Heat and Mass Transfer*, *55* (2012), 15-16, pp. 3921-3932

[40] Steinke, M. E., Kandlikar, S. G., Single-Phase Liquid Friction Factors in Micro-Channels, *International Journal of Thermal Sciences*, *45* (2006), 11, pp. 1073-1083
[41] Patlazhan, S., Vagner, S., Apparent Slip of Shear-Thinning Fluid in a Micro-Channel with a Superhydrophobic Wall, *Physical Review E*, *96* (2017), 1, 013104
[42] Choi, C.-H., *et al*., Effective Slip and Friction Reduction in Nanograted Superhydrophobic Micro-Channels, *Physics of Fluids*, *18* (2006), 8, 087105

Paper submitted: September 1, 2022
Paper revised: November 2, 2022
Paper accepted: November 18, 2022